

Adsorption of Aqueous Using Granular Adsorbents from *Accanthospermum hispidum* DC

Sunusi A. Zubair¹, Umar Ibrahim Gaya^{1*}

¹Department of Pure and Industrial Chemistry, Faculty of Physical Sciences, Bayero University, Kano, 700241, NIGERIA

*Corresponding Author

DOI: <https://doi.org/10.30880/jst.2021.13.01.003>

Received 30 December 2020; Accepted 7 April 2021; Available online 20 April 2021

Abstract: Granular activated carbons have been important adsorbents for the decontamination of aqueous environmental contaminants. *Acanthospermum hispidum* weed represents a ready available source of low-cost adsorbents in sub-Saharan Africa that has barely been paid attention. The effects of pH, contact time, concentration, adsorbent dosage, particle size and temperature on the adsorptive removal of Pb (II) from aqueous solutions over activated carbon granules from the thorns of *Accanthospermum hispidum* (AC-T) were for the first time investigated and compared with those of the leaves (L), the sodium hydroxide modified thorns (NaOH-T) and regular thorns (T) of this plant. These adsorbents were characterised by the surface charge analysis, scanning electron microscopy (SEM) and the Attenuated Total Reflectance Fourier Transform infrared (ATR FTIR) spectroscopy. The SEM revealed a wafer-like appearance for the AC-T with a large distribution of open pores. The adsorption data of lead uptake onto the adsorbents were examined using two pseudo-order kinetic schemes and three isotherm models. To fully understand the adsorption capacities of the adsorbents, batch desorption recoveries were studied. The FTIR depicted the various functionalities responsible for the adsorption. Adsorption over AC-T was found to agree with pseudo second-order kinetic scheme, the Langmuir and Freundlich isotherm. This material exhibited the highest adsorption capacity. The order of reusability of the adsorbents is T < AC-T < NaOH-T.

Keywords: *Accanthospermum hispidum*, lead, sorption, isotherm

1. Introduction

Water quality is key to human health and essential to life. At present, the various societies are facing exponential increase in health risks due to hiking industrial and agricultural development that is invariably associated with uncontrolled anthropogenic release of alarming levels of trace heavy metals to the aqueous environment (Islam et al., 2015; Patel et al., 2017; Cengiz et al., 2017). The Pb²⁺, along with cadmium and mercury, make the top of the “big three” heavy metal pollutants associated with poisoning (Liu et al., 2011). Inevitably, the chemical, biological and physical characteristics of water must be kept within acceptable limits.

Several technologies have been investigated for the removal of heavy metals from aqueous environment which include oxidation/reduction, coagulation-flocculation, cementation, membrane filtration, precipitation, solvent extraction, adsorption and ion exchange (Dehghani, 2015; Kalavathy and Miranda, 2010). Even though the applicability of photocatalytic oxidation of arsenite (As³⁺) to less toxic arsenate (As⁵⁺) has been demonstrated (Li et al., 2009), the mechanism has yet to be understood and, apart from arsenite, only a few other metal ions have been abated by this technology (Gaya et al., 2014). Evidently, adsorption stands in the forefront due to its low cost of operation, effectiveness and wide choice of adsorbents (Varga et al., 2013).

The choice of adsorbent is one of the factors that dictate the efficiency of the sorption process. Consequently, a high number of adsorbents continually emerge from various sources including aquatic plants, fruit peels, shells and nuts,

bagasse, cob, metal oxides, cellulose, graphene based nanocomposites, activated carbons and carbonaceous materials (Sathishkumar et al., 2009; Keskinan et al., 2003; Author et al., 2015; Bagbi et al., 2017; Xu et al., 2017, Sherlala et al., 2018). In this work, we aimed to study for the first time, the adsorption of Pb(II) onto *Accanthospermum hispidum*-based granular adsorbents. This plant grows as a weed and is commonly available in sub-Saharan Africa. We undertake to investigate and compare the adsorption behaviours of the various adsorbents from this material. The choice of granular type of activated carbons was based on the fact that they can be easily prepared from waste plant biomass (Ahmad and Hameed, 2010) and can outperform many porous carbonaceous adsorbents in terms of adsorption capacity, including single and multi-walled carbon nanotubes (Zhang et al., 2010).

2. Materials and Methods

2.1 Chemicals

Chemicals used in this study include hydrochloric acid (HCl; Sigma Aldrich, 37%), nitric acid (HNO₃; BDH, 69%), sodium hydroxide (NaOH; BDH, 97.5%), potassium nitrate (KNO₃; M and B, 89%), calcium chloride (CaCl₂; M and B, 95%), ethanol (Merck, 99%) and lead nitrate (Pb(NO₃)₂; Burgoyne, 99%). All preparations were performed in deionised water.

2.2 Adsorbent Preparation

Samples of *Accanthospermum hispidum* DC was collected from irrigation farmlands about Dambo dam, Kazaure Local Government Area, Jigawa state, Nigeria. The plant was identified and certified at the herbarium of the Department of Plant Biology, Bayero University, Kano. It was dried under shade and later on separated into the thorns and the leaves. Features of the leaves and thorns are shown in Fig. 1.

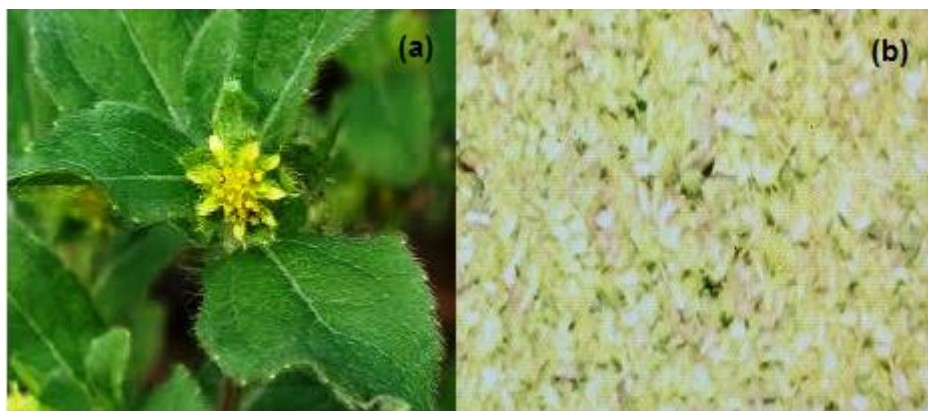


Fig. 1 - Parts of the precursor plant, *Accanthospermum hispidum* DC. (a) The leaves; (b) the thorns

In this study, four adsorbents have been prepared. The thorns (or leaves) (300g) of the plant were washed thoroughly with tap water to remove dirt, rinsed with deionised and finally dried in an electrical oven at 105°C overnight. Oven dry thorns (or leaves) were then divided into three portions. The first portion was ground and sieved into different granular particle sizes (≤ 150 , ≤ 212 , ≤ 300 , ≤ 425 and ≤ 600) μm using Endecott electric sieve. The resulting fractions were collected, stored in airtight plastic containers and labelled as T (or L) and used directly in the adsorption experiments.

The NaOH-modified *A hispidum* thorns (NaOH-T), was prepared by modification of T using a previously described method (Ning-chuang and Xue-yi, 2012). Exactly 100 g of the dried T was soaked in a solution containing ethanol (500 ml), NaOH (250 ml; 0.8 mol/l) and CaCl₂ (250 ml; 0.8 mol/l) for 20 hours. The modified T was washed and filtered repeatedly with plenty water until pH 7. It was then rinsed with deionised water and oven-dried overnight at 105°C. The resulting material was ground, sieved into particle sizes (≤ 150 , ≤ 212 , ≤ 300 , ≤ 425 and ≤ 600) μm and stored in airtight plastic containers labelled (NaOH-T) as the third adsorbent. To prepare the fourth adsorbent, 90g of the dry T was heated at 350°C for one hour in an electric muffle furnace, allowed to cool in the furnace for three hours before final cooling in a desiccator. This carbonized material was mixed with pellets of sodium hydroxide at an impregnation ratio of 1:3 and heated again for one hour at 350°C in order to corrode the surface of the carbonized. It was then washed with plenty of water until pH 7, rinsed with deionised water and dried overnight in an oven at 105°C. The final material was then ground using a clean pestle and mortar, sieved into granular particle sizes (≤ 150 , ≤ 212 , ≤ 300 , ≤ 425 and ≤ 600) μm and stored in plastic containers and labelled as AC-T.

2.3 Batch Adsorption Experiments

In order to determine the effect of operating variables, batch adsorption experiments were carried out in 250 ml batch reactor with one parameter varied while other variables were fixed. The effect of contact time and the adsorbent particle sizes were investigated in the range of 10 to 180 min and 150-600 μm , respectively. Initial Pb(II) concentrations were varied within 25-300 mg/l at desired pH (1, 2, 4, 6, 8 or 10). The adjustment of the system's pH carried out using equimolar NaOH and HNO₃. Adsorbents (4-30 mg/l) were mechanically dispersed by stirring at 200 rpm. The effect of temperature was studied at 303, 313, 323 and 333 K. Test samples were withdrawn at regular time intervals and filtered using watchman filter paper (Cat. No. 1001-125). The absorbance of these test samples was measured using BUCK Scientific, model number 210 VGP Atomic Absorption Spectrophotometer. The concentration of each test sample C_e was extrapolated from calibration curves. The % adsorption and amount of metal adsorbed on the adsorbent were calculated by using Eq. (1) and Eq. (2):

$$\% \text{ adsorption} = \left(\frac{C_o - C_e}{C_o} \right) \times 100 \quad (1)$$

$$q_e = V \left(\frac{C_o - C_e}{w} \right) \quad (2)$$

Where C_o is the initial concentration of metal ion (mg/l), C_e is the concentration the metal ion when equilibrium is reached (mg/l), q_e is the amount of metal ion adsorbed (mg/g), V is the volume of the solution in litre and w is the weight (g) of the adsorbent. The optimum values of operating variables were used to determine possible consistence with a given kinetic scheme. Similarly, the data obtained from the effect of temperature permitted the estimation of thermodynamic functions.

2.4 Desorption Experiments

The strength of adsorption can also be measured based on the amount of the desorbed Pb(II). The desorption was determined using the method of Saeed et al. (2005) by dissolving 1 g of loaded adsorbent into 50 ml of 0.1 mol/l HCl and agitated for 1 h. The suspension was filtered and the residue was carefully allowed to dry for use again. The process was repeated five times. Absorbance was measured using UV-Vis spectrometer.

2.5 Percent Moisture

Moisture (%) was determined directly using OHAUS MB23 moisture analyser equipped with an infra-red heat source.

2.6 Surface Charge Analysis

In order to determine the pH at which the adsorption may be very effective, the point of zero charge of the adsorbent was determined using the method of Banerjee et al. (2012). To permit proper comparison, the pH at point of zero charge (pH_{pzc}) was determined for the adsorbents from the thorns. Aliquot (45 ml) of 0.1 mol/l KNO₃ solution was transferred into 250 ml conical flasks and pH was adjusted to 2, 4, 6, 8, 10 or 12. The content in each flask was then made to exactly 50 ml by dropwise addition of the KNO_{3(aq)}} and the pH was measured again and noted as pH_i . The adsorbent (1 g) was immediately dispersed into each flask and agitated at 303K and 200 rpm for 1 h. The suspension was filtered using Whatman filter paper and the pH of the supernatant solution was measured and noted as pH_f . The difference between the pH_i and the pH_f (or ΔpH) was plotted against pH_i . The point of zero charge corresponds to the point of intersection of the abscissa at $\Delta\text{pH} = 0$.

2.6 Scanning Electron Microscopy and Infrared Spectroscopy

In order to provide insight into the characteristics of the adsorbents scanning electron microscopy (SEM) and Fourier Transform infrared (FTIR) spectroscopy were performed before and after adsorption. The surface morphologies of the adsorbents were imaged using SEM Leica 440 instrument at accelerating voltage and magnification of 10 kV and 500 \times , respectively. Fourier Transform infrared (FTIR) spectroscopy was performed on Agilent Cary 630 Attenuated Total Reflectance (ATR) FTIR in the wave number range of 4000 to 400 cm^{-1} and background scan rate of 32.

3. Results and Discussion

3.1 Properties of the Adsorbent Surface

The SEM micrograph of *Accanthospermum hispidum* activated carbon (AC-T) before and after adsorption of Pb(II) are displayed in Fig. 2. The image of this adsorbent only shows a wafer-like formation (Fig. 2a), which does not physically differ from the morphology after adsorption (Fig. 2b).

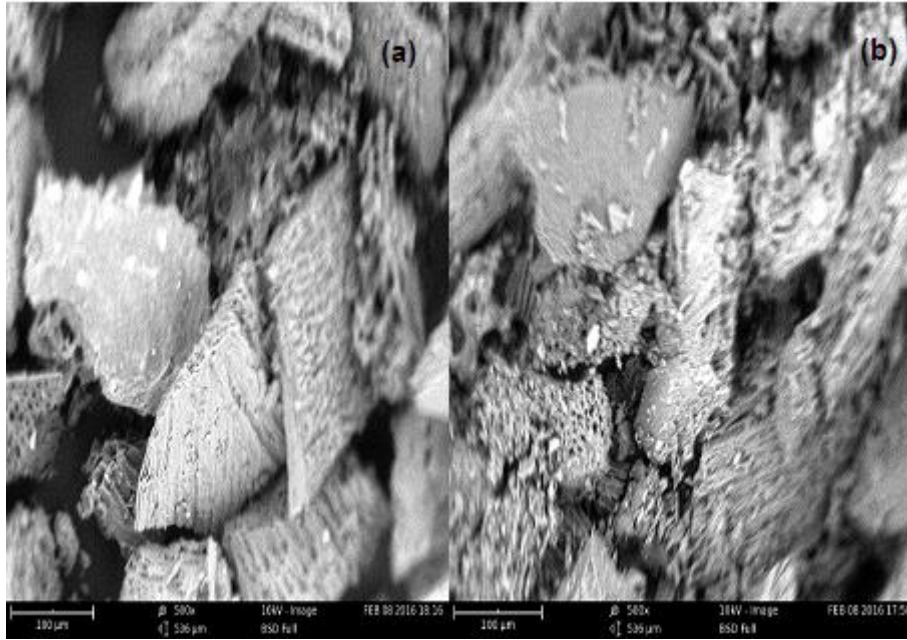


Fig. 2 - The SEM micrographs of AC-T (a) before Pb (II) removal; (b) after adsorption of Pb(II)

The FTIR spectra of the activated carbon of *Accanthospermum hispidum* thorns (AC-T) were recorded before and after adsorption. Bands were observed at 2922, 2851, 1104 and 748 cm^{-1} prior to lead adsorption (Fig. 3a) which could be assigned to alkyl -C-H , -O-H , -C-O and -C-H bending respectively (Ning-Chuang *et al.*, 2010). The band 1776 cm^{-1} correspond to carbonyl -C=O stretching vibration. The shift observed in the intensities of these peaks after Pb(II) adsorption, though negligible (Fig. 3b), indicate chemical adsorption.

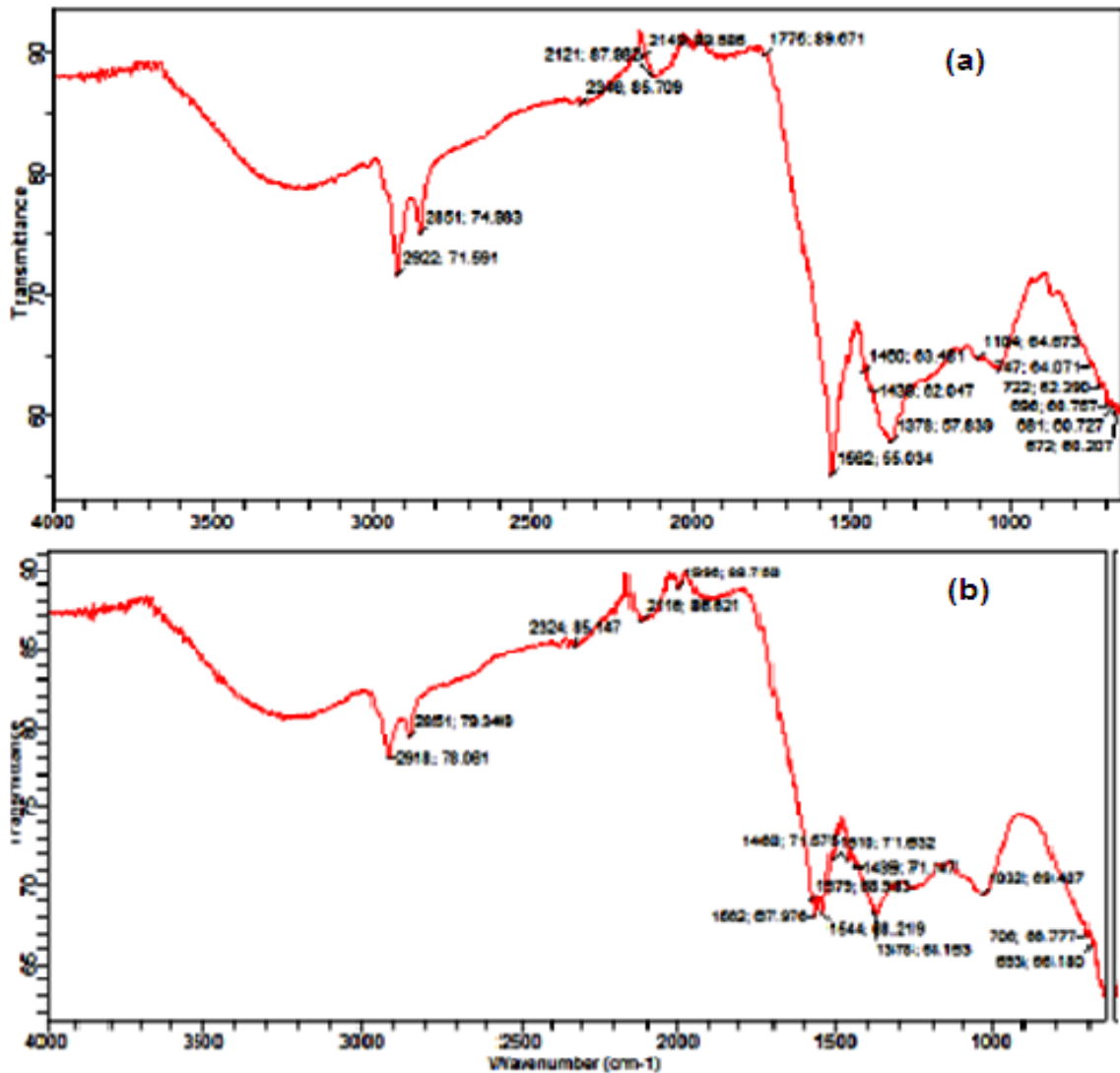


Fig. 3 - The FTIR bands of AC-T (a) Prior to Pb(II) adsorption; (b) After Pb(II) adsorption

Moisture is an important characteristic of adsorbents that cannot be overstressed. The results of their analysis for *Accanthuspermum hispindum* adsorbents are shown in Table 1. As seen from the table, the activated carbon powder (AC-T) had the lowest moisture (5 %), followed by NaOH-T (5.5), T (5.7) and L (6.8), respectively. Basically, the lower the moisture content of adsorbents the better the adsorption capacity. A limit of 15 % has been specified for activated carbon by the Indonesian Industrial Standard (SII No. 0258-88) (Zulkania et al., 2018). This corroborates why AC-T is the most active adsorbent.

To understand how surface charge can affect the adsorption equilibrium, point of zero charge pH was determined. A list of the pH at point of zero charge (pH_{pzc}) of the adsorbents used in this study is displayed by Table 1. A sample of the pH profile for the AC-T is displayed by Fig. 4 (See also those of NaOH-T and T in the supplementary file; Figures 1S and 2S). From this table there is no significant change in the pH at point of zero charge (pH_{pzc}) as the thorns adsorbent (T) is converted to NaOH-T or AC-T. Generally therefore, below pH 6 the uptake of the positively charged Pb(II) will decrease due to repulsion. Conversely, the uptake of $\text{Cr}_2\text{O}_7^{2-}$ will increase due to enhanced electrostatic attraction. The pH_{pzc} of the granular thorns T is the same as that reported for watermelon rind adsorbent (Banerjee et al., 2012).

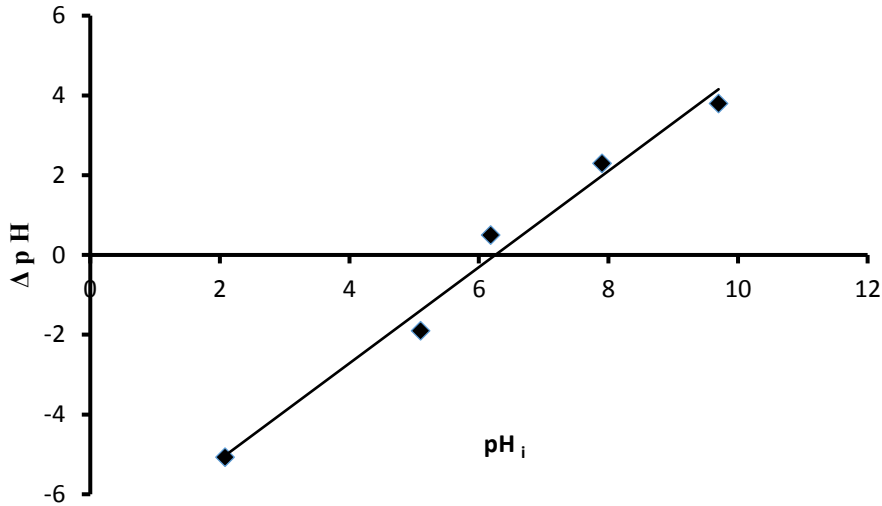


Fig. 4 - Point of zero charge plot for AC-T

Table 1 - General properties of the adsorbent

Property	L	T	NaOH-T	AC-T
Moisture content (%)	6.8	5.7	5.5	5
Point of zero charge	ND ^a	6	6.3	6.2

a = Not determined

3.2 Effect of Adsorption Variables and Kinetics

The effect of operating parameters is depicted by the profiles in Fig. 5. Solution pH is the main factor affecting the rate of adsorption as it affects the chemistry of both functional groups and metal ions (Saeed *et al.*, 2005). Figure 5a shows the effect of pH on the adsorptions of Pb (II) over AC-T, NaOH-T, T and L. From the figure Pb(II) uptake onto AC-T was 7.68 mg/g at pH 1 but at pH = 6 (corresponding to the optimum pH) the uptake increased to the maximum value of 11.13 mg/g (95 %). The pH 6 was previously reported to be optimum for the removal of the same metal using onion skin adsorbents (Saka *et al.*, 2011). Similarly, the optimum pH for the removal of lead over the adsorbent L is 6, and at this pH up to 4.70 mg/g (94 %) lead is removed. For NaOH-T, the optimum pH is 8, with 89.5% removal and 11.27 mg/g of the metal in the adsorbed phase. The leaves (T) adsorbed 4.63 mg/g lead up to 6.83 mg/g between pH 1 and 6. The adsorption remained steady up to pH 8 and then decreased due to excess concentration of the adsorbent.

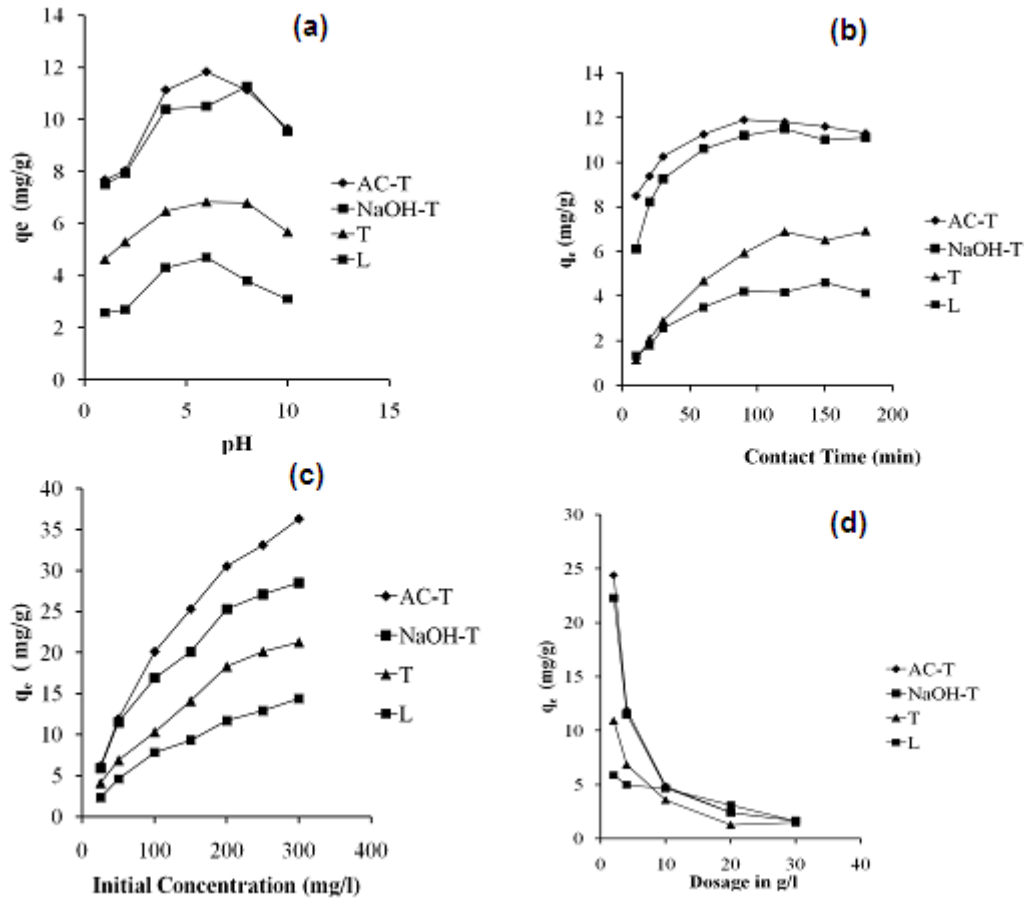


Fig. 5 - Plots of the variation of adsorption capacity of Pb(II) with (a) pH; (b) contact time; (c) initial concentration; (d) adsorbent dosage

The influence of contact time on the removal of Pb(II) by all the adsorbents is shown by Fig. 5b. It is readily seen from the figure that the activated carbon (AC-T) attained equilibrium rather rapidly within the 90 min corresponding to 11.9 mg Pb(II)/g and 95 % lead removal. As no significant change in the equilibrium times was observed, subsequent experiments were therefore performed for this equilibrium time. The equilibrium contact time depends upon the adsorbent, metal and concentrations used in the experiment (Kalavathy and Miranda, 2010). Consequently, the NaOH-T adsorbed only 92 % of the Pb(II) (equivalent to 11.5 mg/g) in 120 min. Even though the contact time for lead adsorption over the T was also 120 min, only 55.6 % (6.83 mg/g) lead was removed. For the L, the uptake of the metal was observed to rise steadily until maximum uptake was reached at 150 minutes, thereafter, the uptake remained constant with increasing contact time. The highest percentage removal and the corresponding quantity of the metal adsorbed were 93 % and 4.6 mg/g respectively. Therefore 150 minutes is recommended for the adsorption of lead over the adsorbent L.

The influence of concentration on the removal of Pb (II) ions is displayed by Fig. 5c. Generally, irrespective of the adsorbent, the higher the initial concentration of the higher the amount of metal adsorbed. This unique property of the adsorbents within the concentration regimes of the study (25 to 300 mg/l) may be attributed to the presence of a large number of open pores on the adsorbents surfaces (Fig. 5c). For example, the uptake capacity of Pb (II) by the AC-T was 6.13 mg/g when the initial concentration is 25 mg/l and this rose steadily up to 36.3 mg/g as concentration reached 300 mg/l. The order of decreasing lead uptake is AC-T > NaOH-T > T > L.

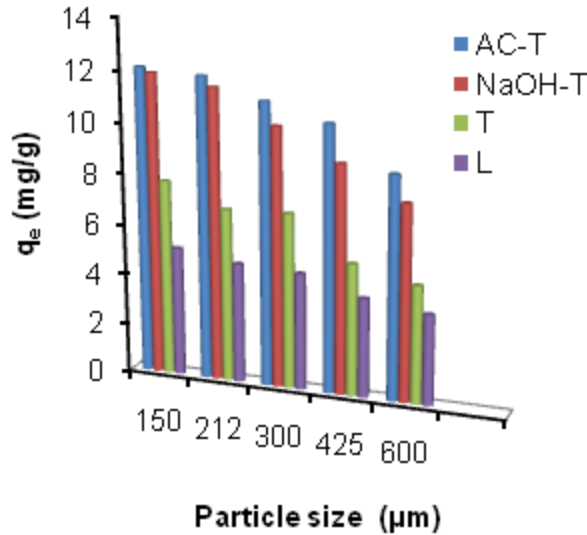


Fig. 6 - Variation of amounts of adsorbed lead with particle size

The effect adsorbent dosage on the removal of Pb(II) was monitored at pH 6, is depicted by Fig. 5d. From the figure, the uptake of Pb(II) by AC-T rose sharply from 24.4 to 11.9 mg/g (89.8 to 95.4 % removal) as the adsorbent dosage is varied from 2 g/L to 4 g/L (or 0.1 to 0.2 g). This uptake diminished to 1.61 with further increase in the adsorbent dosage down to 30 g/l (or 1.5 g). Therefore, 4 g/L was considered as the optimum adsorbent dosage. Accordingly within the remaining adsorbents behaved in a similar manner with increase in adsorbent doses. At the other end, the effect of granular adsorbent size range (150 to 600 µm) on the lead adsorption capacity was investigated (Fig. 6). From the figure an increase in the particle size from ≤ 150 µm to ≤ 600 µm caused a decrease in the quantity of the AC-T adsorbed lead from 12.1 to 8.75 mg/g (96.2 to 69.8 % removal). From analytical standpoint, adsorption was nearly steady up to ≤ 212 µm corresponding to 11.9 mg/g (95.4 % removal). Therefore, particle size of ≤ 212 µm was considered as optimum for the Pb(II) removal. As the particle size is increased down to ≤ 600 µm the quantity of the metal adsorbed decreased from to 8.75 mg/g 69.8 % removal. Similar trend was observed for NaOH-T, T and L. The negative effect of particle size can be attributed to the decrease in surface area which results in decreased sites for adsorption.

3.3 Isotherms and Adsorption Kinetics

The adsorption data of Pb(II) were tested against Langmuir, Freundlich and Temkin two-parameter isotherm models and the resulting data are displayed in Table 2 (see also isotherms in the supplementary Fig. 3-6). The Langmuir adsorption isotherm is given by Equation (3).

$$\frac{C_e}{q_e} = \frac{1}{q_{max} K_L} + \frac{C_e}{q_{max}} \quad (3)$$

Where, C_e is equilibrium concentration (mg/l), q_e is amount of metal adsorbed (mg/g), q_{max} is the maximum adsorption (mg/g) which gives a complete monolayer and K_L is the adsorption equilibrium constant in l/mg. A linear plot of C_e/q_e against C_e gives a slope of $1/q_{max}$ and an intercept of $1/K_L q_{max}$. As may be seen from Table 2, the highest value of q_{max} (38.5 mg/g) was obtained when AC-T was applied as adsorbent. This value is slightly less than the q_{max} (46.69 mg/g) reported for the removal of Pb(II) using *Myriophyllum spicatum* as adsorbent (Keskinan et al., 2003).

The Freundlich model is based on Eq. (4).

$$\log q_e = \log K_F + \frac{1}{n} \log C_e \quad (4)$$

Where n (dimensionless) characterizes the adsorption strength and K_F is the Freundlich constant. The K_F value relates to bond strength and increases with the total adsorption capacity of the adsorbent. A linear plot of $\log q_e$ against $\log C_e$ gives a straight line with a slope $\frac{1}{n}$ (whose value is indicative of bond energies between the metal ion and the adsorbent), and intercept of $\log K_F$. From Table 2 the uptake of Pb(II) over all the adsorbents used in this study is associated with high n values (or low $1/n$ values) which translate to stronger the interaction between the adsorbents and the heavy metal (Jonathan et al., 2009). The Temkin isotherm is given by Eq. (5).

$$q_e = \frac{RT}{B} \ln A + \frac{RT}{B} \ln C_e \quad (5)$$

Where A (l/g) and B are Temkin constants whose values are obtained from intercept and slope of the plot of q_e against $\ln C_e$, respectively. Generally speaking, the adsorption processes are consistent with Langmuir isotherm, except for AC-T whose adsorption was consistent with both Langmuir and Freundlich isotherm rather than the Temkin isotherm as demonstrated by the high R-square values in the former cases (Table 2). Agreement with both of these isotherms was previously reported for Pb(II) adsorption on carbon nanotube (Li et al., 2003) and potassium hydrogen phthalate adsorption on TiO₂ (Valente et al., 2006). The agreement of our data with Langmuir isotherm is supportive of the chemisorption mechanism, which informs of the high binding energy between Pb(II) and the adsorbents.

Table 2 - Parameters of selected isotherms for the removal of 50 mg/l Pb (II) at pH 6

Adsorbent (4 g/l)	Langmuir			Freundlich			Temkin		
	R ²	q_{max} (mg/g)	K_L	R ²	K_F (mg/g)	1/n	R ²	A	B
AC-T	0.994	38.5	0.556	0.996	9.31	0.266	0.955	5.59	5.66
NaOH-T	0.976	31.3	0.080	0.908	7.53	0.260	0.909	4.47	3.75
T	0.947	26.3	0.014	0.899	26.3	0.004	0.949	6.95	-16.1
L	0.973	17.2	0.002	0.987	2.98	0.305	0.945	5.23	-14.2

The kinetics of Pb(II) removal was evaluated using the Lagergren pseudo first-order equation [Eq. (6)] and the pseudo second-order equation [Eq. (7)].

$$\ln(q_e - q_t) = \ln q_e - k_1 t \quad (6)$$

$$\frac{t}{q_t} = \left(\frac{1}{k_2 q_e^2} + \frac{t}{q_e} \right) \quad (7)$$

Where q_e and q_t are the adsorption capacities at equilibrium and at any time t , respectively. The k_1 in Eq. (6) is the pseudo first-order rate constant whose value is obtained as the slope of $\ln(q_e - q_t)$ versus t . The k_2 in Eq. (7) can be obtained from the plot of t/q_t versus t whose intercept is $1/k_2 q_e^2$. The calculated and experimental adsorption capacities as well as the pseudo first-order and pseudo second-order rate constants are displayed in Table 3 (with representative kinetic profiles in the supplementary (Fig. 6-9)). From the table, it can be seen that the Pb(II) adsorption is more consistent with the pseudo second-order kinetic model, which reveals chemical adsorption. This is further confirmed by the values of correlation coefficients (which are all close to unity) and the fact that experimental and calculated adsorption capacities do not differ significantly. The pseudo second-order kinetic scheme shows that the adsorption is chemisorption-controlled.

Table 3 - Kinetic data for the removal of Pb(II) from 50 mg/l solution at pH 6

Adsorbent (4 g/l)	Observed q_e (mg/g)	Pseudo-first order equation			Pseudo-second order equation		
		R ²	Calculated q_e (mg/g)	k_1 (min ⁻¹)	R ²	Calculated q_e (mg/g)	k_2 (g/mg min)
AC-T	11.9	0.984	4.05	0.0299	0.998	12.2	0.0175
NaOH-T	11.5	0.913	6.68	0.0386	1.000	12.6	0.0074
T	6.83	0.986	6.65	0.0207	0.999	12.5	0.0007
L	4.60	0.995	3.24	0.0161	0.996	5.43	0.0057

The performances of all the adsorbents for the uptake of Pb(II) were evaluated by adsorption and desorption over the thorn-based adsorbents for five cycles. The essence of desorption experiments is to understand how the Pb(II) ion is transferred between aqueous phase and adsorbent phase, whether in exchangeable, complexed or adsorbed form and if more than the adsorption process (Xie et al., 2018). The uptake of the lead by these adsorbents in the last cycle was used to grade the efficiencies of the adsorbents. The lead desorption profiles are displayed in Fig. 7. From the figure, the quantity of the Pb(II) in the adsorbed-phase after 5 cycles of use of the adsorbents T, AC-T and NaOH-T are 9.25 mg/g,

9.90 mg/g and 10.4 mg/g which shows the order of reusability T < AC-T < NaOH-T, respectively. This order can be attributed to the increasing order of affinity of Pb(II) to the surface of the adsorbents.

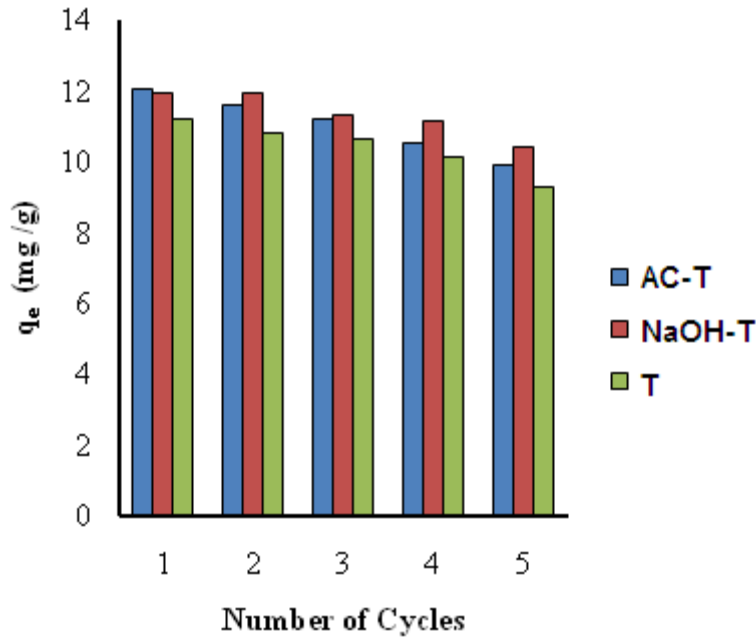


Fig. 7 - Profiles of Pb(II) desorption from thorns adsorbents

3.4 Thermodynamics

Thermodynamic functions were determined from experimental data obtained at 303, 313, 323 and 333 K. The heterogeneous equilibrium constant K for the adsorption equilibria is given by the Eq. (8).

$$K = \frac{C_s}{C_e} \tag{8}$$

$$\Delta G^\circ = -RT \ln K \tag{9}$$

Where C_s (mg/l) is the amount of adsorbate in the adsorbed phase and C_e (mg/l) is the equilibrium concentration of the solution. The values of K for Pb(II) adsorption onto the adsorbents used in the study were calculated. The corresponding values of the Gibbs free energy change (ΔG°) were calculated using Eq. (9). The thermodynamic functions such as adsorption enthalpy (ΔH°) and entropy change (ΔS°) are given by the Eq. (10).

$$\ln K = -\frac{\Delta H^\circ}{RT} + \frac{\Delta S^\circ}{R} \tag{10}$$

Table 4 - Thermodynamic data for the removal of Pb(II) from 50 mg/l solution at pH 6

Adsorbent	ΔG (kJ/mol)				ΔH (kJ/mol)	ΔS (J/mol K)
	303 K	313 K	323 K	333 K		
AC-T	-4.01	-2.71	-1.41	-0.11	-43.4	-130
NaOH-T	-3.43	-2.51	-1.59	-0.66	-31.4	-92.3
T	+2.92	+3.47	+4.03	+4.58	-13.9	-55.5
L	-0.53	-1.12	-1.83	-2.48	+19.2	+65.1

The activation energies of adsorption over the *Accanthuspermum hispidum* adsorbents are shown in Table 4. From the table, the negative Gibbs free energies for the adsorption of Pb(II) over AC-T, NaOH-T and L were consistent and this shows the feasibility and the spontaneous nature of these adsorption processes (Sathishkumar et al., 2009). However, for the Pb(II) removal on the surface of the adsorbent T negative values of ΔS and ΔH with a positive ΔG indicate the need for lower temperatures for the process to proceed spontaneously. Conversely, the positive ΔS and ΔH values associated with the adsorption over L indicate the need for higher temperatures for the process to be spontaneous.

3.5 Correlation of Surface Properties with Performance

Some many factors may be considered responsible for the performance of the *Accanthuspermum hispidum* –based adsorbents. They demonstrated low moisture, favourable pH_{pzc} and surface functionalities such as $-O-H$, $-C-O$ and $-C=O$ which may be sufficient to account for the observed efficiency of adsorption. Since chemical adsorption mechanism holds true, these functional groups may mediate in monolayer formation and lead binding affinity. The point of zero charge pH obtained for the thorn-based adsorbents were all above 6 which reveal the non-suitability of the adsorbents for use in acidic media.

Conclusion

This study successfully shows the effectiveness of granular adsorbents generated from readily available *Accanthuspermum hispidum* weed for the adsorptive removal of Pb(II) from aqueous solutions. The adsorption was observed to be dependent on pH, contact time, concentration, temperature and particle size. The pH at the point of zero charge appeared as important factor that dictates the adsorption equilibrium.

Acknowledgement

Sunusi Zubair acknowledges the Muhammad Shehu Ismail of Civil Engineering of Bayero University for facilitating the use of Endecott electric Sieve.

References

- [1] Ahmad, A.A., & Hameed, B.H. (2010). Fixed-bed adsorption of reactive azo dye onto granular activated carbon prepared from waste. *Journal of Hazardous Materials*. 175, 298–303
- [2] El-Ashtoukhy, E.S.Z., Amin, N. K., & Abdelwahab, O. (2008). Removal of lead (II) and copper (II) from aqueous solution using pomegranate peel as a new adsorbent. *Desalination*. 223, 162–173
- [3] Bagbi, Y., Sarswat, A., Mohan, D., Pandey, A., & Solanki, P.R. (2017). Lead and chromium adsorption from water using L-Cysteine functionalized magnetite (Fe_3O_4) nanoparticles. *Scientific Reports*. 7, 7672
- [4] Banerjee, K., Ramesh, S.T., Gandhimathi, R., Nidheesh, P.V., & Bharashi, K. S. (2012). A novel agricultural waste adsorbent, watermelon shell for the removal of copper from aqueous solutions. *Iranica Journal of Energy and Environment*. 3(2), 143-156
- [5] Cengiz, M.F., Kilic, S., Yalcin, F., Kilic, M., & Yalcin, M.G. (2017). Evaluation of heavy metal risk potential in Bogacayi River water (Antalya, Turkey). *Environmental Monitoring and Assessment*. 189(6), 1-12
- [6] Dehghani, M.H., Taher, M. M., Bajpai, A. K., Heibati, B., Tyagi, I., Asif, M., et al. (2015). Removal of noxious Cr (VI) ions using single-walled carbon nanotubes and multi-walled carbon nanotubes. *Chemical Engineering Journal*. 279, 344–352
- [7] Kalavathy, M.H., & Miranda, L.R. (2010). Moringa oleifera-A solid phase extractant for the removal of copper, nickel and zinc from aqueous solutions. *Chemical Engineering Journal*. 158, 188–199
- [8] Keskinan, O., Goksu, M.Z.L., Yuceer, A., Basibuyuk, M., & Forster, C.F. (2003). Heavy metal adsorption characteristics of a submerged aquatic plant (*Myriophyllum spicatum*), *Process Biochemistry*. 39, 179-183
- [9] Li, Q., Easter, N. J., & Shang, J. K. (2009). As(III) removal by palladium-modified nitrogen-doped titanium oxide nanoparticle photocatalyst. *Environmental Science and Technology*. 43, 1534–1539
- [10] Li, Y. H., Wang, S., Luan, Z., Ding, J., Xu, C., Wu, D. (2003). Adsorption of cadmium(II) from aqueous solution by surface oxidized carbon nanotubes. *Carbon*. 41, 1057-1062
- [11] Liu, W.-J., Zeng, F-X., Jiang, H., Zhang, X.-S., & Yu, H.-Q. (2011). Techno-economic evaluation of the integrated biosorption–pyrolysis technology for lead (Pb) recovery from aqueous solution. *Bioresource Technology*. 102(10), 6260-6265
- [12] Gaya, U.I. (2014). *Heterogeneous photocatalysis using inorganic semiconductor solids*. Springer, Dordrecht
- [13] Gaya, U.I., Otene, E., & Abdullah, A.H. (2015). Adsorption of aqueous Cd(II) and Pb(II) on activated carbon nanopores prepared by chemical activation of doum palm shell. *SpringerPlus*. 4, 458
- [14] Islam, M.S., Ahmed, K., Raknuzzaman, M., Habibullah-Al-Mamun, M., & Islam, M.K. (2015). Heavy metal pollution in surface water and sediment: A preliminary assessment of an urban river in a developing country. *Ecological Indicators*. 48, 282–291
- [15] Jonathan, F., Aline, N. K., Jaka, S., Yi-Hsu, J., Nani, I., & Suryadi, I. (2009). Equilibrium and kinetic studies in adsorption of heavy metals using biosorbent: A summary of recent studies. *Journal of Hazardous Materials*. 162, 616–645
- [16] Ning-chuan F., Guo, X., & Liang S. (2010). Enhanced Cu (II) adsorption by orange peel modified with sodium hydroxide. *Transactions of Nonferrous Metals Society of China*. 20, 146-152

- [17] Patel, P., Raju, N.J., Reddy, B.C.S.R., Suresh, U., Sankar, D.B., & Reddy, T.V.K. (2018). Heavy metal contamination in river water and sediments of the Swarnamukhi River Basin, India: risk assessment and environmental implications. *Environmental Geochemistry and Health*. 40(2), 609-623
- [18] Saeed, A., Waheed, M. A., & Muhammed, I. (2005). Removal and recovery of heavy metals from aqueous solution using papaya wood as a new biosorbent. *Separation and Purification Technology*. 45, 25-31
- [19] Saka, C., Sahin, O., Demir, H., Kahyagoglu, M. (2011). Removal of lead from aqueous solutions using preboiled and formaldehyde treated onion skins as a new adsorbent. *Separation. Science Technology*. 46, 507- 517
- [20] Sathishkumar, M., Binupriya, A. R., Kavitha, D., Selvakumard, R., Jayabaland, R., Choie, J. G., et al. (2009). Adsorption potential of maize cob carbon for 2,4-dichlorophenol removal from aqueous solutions: Equilibrium, kinetics and thermodynamics modeling. *Chemical Engineering Journal*. 147, 265–271
- [21] Sherlala, A.I.A., Raman, A.A.A., Bello, M.M., & Ashgar, A. (2018). A review of the applications of organo-functionalized magnetic graphene oxide nanocomposites for heavy metal adsorption. *Chemosphere*. 193, 1004-1017
- [22] Sluiter, A., Hames, B., Ruiz, R., Scarlata, C., Sluiter, J., & Templeton, D. (2005). Determination of ash in biomass: Laboratory analytical procedure (LAP, Technical report: NREL/TP-510-42622, January 2008). United States of America: National renewable energy laboratory, U.S. Department of Energy
- [23] Smith, K.M., Fowler, G.D., Pullket, S., & Graham, N.J.D. (2009). Sewage sludge-based adsorbents: A review of their production, properties and use in water treatment applications. *Water Research*. 43, 2569-2594
- [24] Valente, J. P. S., Padilha, P. M., Florentino, A. O. (2006). Studies on the adsorption and kinetics of photodegradation of a model compound for heterogeneous photocatalysis onto TiO₂. *Chemosphere*. 64, 1128–1133.
- [25] Varga, M., Takács, M., Zárny, G., & Varga, I. (2013). Comparative study of sorption kinetics and equilibrium of chromium (VI) on charcoals prepared from different low-cost materials. *Microchemical Journal*. 107, 25–30
- [26] Xie, S., Wen, Z., Zhan, H., & Jin, M. (2018). An experimental study on the adsorption and desorption of Cu(II) in silty clay. *Geofluids*. Article ID 3610921. <https://doi.org/10.1155/2018/3610921>
- [27] Xu, Q., Wang, Y., Jin, L., Wang, Y., & Qin, M. (2017). Adsorption of Cu (II), Pb (II) and Cr (VI) from aqueous solutions using black wattle tannin-immobilized nanocellulose. *Journal of Hazardous Materials*. 339, 91–99
- [28] Zhang, Z., Shao, T., Selcen Kose, H., & Karanfil, T. (2010). Adsorption of aromatic compounds by carbonaceous adsorbents: A comparative study of granular activated carbon, fiber and carbon nanotubes. *Environmental Science and Technology*. 44, 6377–6383
- [29] Zulkania, A., Ghina Hanum, F., & Rezki, A.S. (2018). The potential of activated carbon derived from bio-char waste of bio-oil pyrolysis as adsorbent. *MATEC Web of Conferences*. 154, 01029. <https://doi.org/10.1051/mateconf/201815401029>